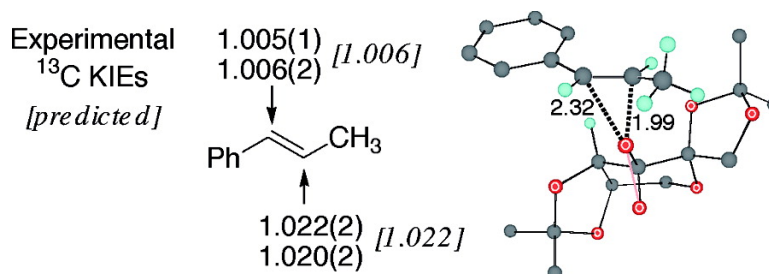


Isotope Effects and the Nature of Enantioselectivity in the Shi Epoxidation. The Importance of Asynchronicity

Daniel A. Singleton, and Zhihong Wang

J. Am. Chem. Soc., **2005**, 127 (18), 6679-6685 • DOI: 10.1021/ja0435788 • Publication Date (Web): 06 April 2005

Downloaded from <http://pubs.acs.org> on March 25, 2009



More About This Article

Additional resources and features associated with this article are available within the HTML version:

- Supporting Information
- Links to the 5 articles that cite this article, as of the time of this article download
- Access to high resolution figures
- Links to articles and content related to this article
- Copyright permission to reproduce figures and/or text from this article

[View the Full Text HTML](#)



Isotope Effects and the Nature of Enantioselectivity in the Shi Epoxidation. The Importance of Asynchronicity

Daniel A. Singleton* and Zhihong Wang

Contribution from the Department of Chemistry, Texas A&M University, P.O. Box 30012, College Station, Texas 77842

Received October 22, 2004; E-mail: singleton@mail.chem.tamu.edu

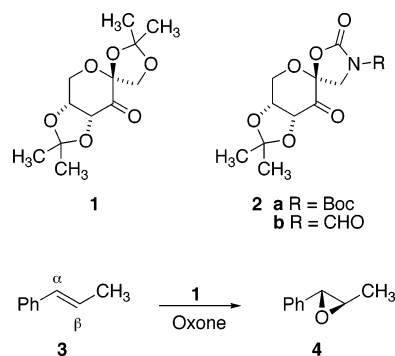
Abstract: The epoxidation of β -methylstyrene catalyzed by the Shi fructose-derived ketone is studied using experimental kinetic isotope effects and DFT calculations. The observation of a large β olefinic ^{13}C isotope effect and small α carbon isotope effect is indicative of an asynchronous transition state with more advanced formation of the C–O bond to the β olefinic carbon. By varying the catalyst conformation and alkene orientation, diverse transition structure geometries were located computationally, and the lowest-energy structure leads to an accurate prediction of the isotope effects. Given this support for the accuracy of the calculations employed, the nature of enantioselectivity in this and related epoxidations is considered. The lowest-energy transition structures are generally those in which the differential formation of the incipient C–O bonds, the “asynchronicity,” resembles that of an unhindered model, and the imposition of greater or less asynchronicity leads to higher barriers. In reactions of *cis*-disubstituted and terminal alkenes using Shi’s oxazolidinone catalyst, the asynchronicity of the epoxidation transition state leads to increased steric interaction with the oxazolidinone when a π -conjugating substituent is distal to the oxazolidinone but decreased steric interaction when the π -conjugating substituent is proximal to the oxazolidinone. Overall, the asynchronicity of the transition state must be considered carefully to understand the enantioselectivity.

Introduction

The rational control of enantioselectivity in a reaction can require a comprehensive knowledge of the reaction mechanism and a detailed geometry of the selectivity-determining transition state. This presents new challenges in efforts to understand chemical reactions. Classical mechanistic tools provide a qualitative picture but usually supply too little detail. The contrasting great detail provided by theoretical calculations has made them an integral tool in studying mechanisms. However, a purely calculational approach faces diverse limitations, particularly for enantioselective reactions. Added to the usual uncertainty as to whether a given theoretical approach is sufficient to represent the basic experimental reaction in solution, most enantioselective reactions involve large chemical systems. This limits the level of applicable theoretical methodology and can greatly increase the conformational complexity of the reaction. For a calculational study leading to a series of transition state conformers, the reliability of the relative energies will be uncertain and it may be unclear whether the best conformer has been found. Under such circumstances, it is very difficult to confidently analyze the nature of the enantioselectivity in a reaction.

Enantioselective oxidations of alkenes provide diverse versatile entries into optically active products. Recent advances in the epoxidation of unfunctionalized alkenes have been particularly impressive.^{1,2} Shi and co-workers have developed one of the most promising of these methodologies.^{2–5} In the Shi enantioselective epoxidation, a chiral ketone derived from fructose, such as **1**, catalyzes the oxidation of alkenes with

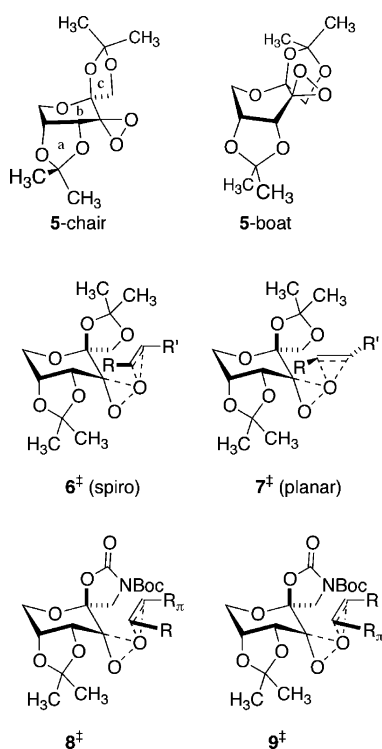
Oxone (potassium peroxydisulfate) as the most common stoichiometric oxidant. An example is the epoxidation of *trans*- β -methylstyrene (**3**) to afford the (+)-(*R,R*) epoxide **4**. The original catalyst **1** is most effective with *trans*-disubstituted alkenes and trisubstituted alkenes, while the oxazolidinone **2a** has been found to be effective with *cis*- and terminal alkenes.^{4,5} The active oxidants are thought to be dioxiranes such as **5**.



Shi has developed explanations of the enantioselectivity in these reactions based on diverse observations. Shi’s model for

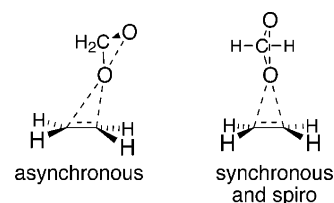
- (1) (a) Jacobsen, E. N.; Zhang, W.; Muci, A. R.; Ecker, J. R.; Deng, L. *J. Am. Chem. Soc.* **1991**, *113*, 7063–7064. (b) Denmark, S. E.; Wu, Z. *Synlett* **1999**, 847–859. (c) Bonini, C.; Righi, G. *Tetrahedron* **2002**, *58*, 4981–5021. (d) Yang, D. *Acc. Chem. Res.* **2004**, *37*, 497–505.
- (2) Shi, Y. *Acc. Chem. Res.* **2004**, *37*, 488–496.
- (3) (a) Tu, Y.; Wang, Z.-X.; Shi, Y. *J. Am. Chem. Soc.* **1996**, *118*, 9806–9807. (b) Wang, Z.-X.; Tu, Y.; Frohn, M.; Zhang, J.-R.; Shi, Y. *J. Am. Chem. Soc.* **1997**, *119*, 11224–11235.
- (4) Tian, H.; She, Z.; Shu, L.; Yu, H.; Shi, Y. *J. Am. Chem. Soc.* **2000**, *122*, 11551–11552.
- (5) Tian, H.; She, Z.; Xu, J.; Shi, Y. *Org. Lett.* **2001**, *3*, 1929–1931.

understanding these reactions starts with a chair conformation of **5** and has the alkene approach the least-hindered equatorial oxygen of the dioxirane. The observed major products can then result from the spiro transition state **6** in which the substituents on a *trans*-disubstituted or trisubstituted alkene are positioned to avoid a steric interaction with the dioxolane c ring. The spiro transition state leading to the minor enantiomer is thought to be sterically unfeasible; instead, the planar transition state **7** is thought to be the main source of the minor enantiomer. For the reactions of *cis*-disubstituted and terminal alkenes catalyzed by **2**, Shi has proposed that the enantioselectivity results from a preference for a π -conjugating substituent (R_π) to be oriented proximal to the oxazolidinone c ring, as in **8**, as opposed to having the π -conjugating substituent away from the oxazolidinone, as in **9**.^{4,5} The origin of this preference has been unclear, although some observations have suggested an attractive interaction between π -conjugating substituents and substituents on the oxazolidinone.²



Theoretical studies of epoxidations mediated by dioxiranes have focused on simple model reactions.^{6–8} These studies have consistently supported a preference for a spiro transition state, as had been deduced from experimental observations.⁹ MP2 and CASSCF calculations favor a transition state for oxidation of ethylene in which there is differential formation of the incipient C–O bonds, describable as highly “asynchronous,” but B3LYP

and several high-level ab initio calculations favor essentially synchronous formation of the two new C–O bonds.^{6,7} In an in-depth study of the reaction of the parent dioxirane with ethylene, Bach ultimately concluded that the potential energy surface is very soft and that an unsymmetrical transition structure is slightly favored.⁷



For such a large system as the Shi epoxidation, the theoretical approach is effectively limited to DFT methods with a moderate basis set, and here the geometry optimizations are carried out using B3LYP calculations with a 6-31G* basis set. Considering the diverging predictions of high-level ab initio calculations, the accuracy of the calculational approach cannot be asserted on theoretical grounds alone. In addition, the use of a single-reference method such as B3LYP for epoxidation calculations has recently been criticized.¹⁰ The reasonable application of these calculations will require validation, and we accomplish this here using kinetic isotope effects (KIEs). The isotope effects provide an experimental basis for assessing the geometrical accuracy of the calculated transition structures. This assessment will support the use of these calculations to examine the origin of the enantioselectivity in these reactions.

Results and Discussion

Experimental Isotope Effects. The prototypical enantioselective epoxidation of **3** catalyzed by **1** was chosen for study. Shi and co-workers have reported that epoxidations of **3** mediated by 30% **1** afforded the (+)-(*R,R*) epoxide **4** in up to 95.7% ee at $-10\text{ }^\circ\text{C}$.^{3b} The epoxidations here using 20% of **1** at $0\text{ }^\circ\text{C}$ afforded at least 92% of the (+)-(*R,R*) enantiomer with an approximately quantitative formation of product.

The ¹³C KIEs for epoxidation of **3** were determined combinatorially by NMR methodology at natural abundance.¹¹ Two reactions of **3** were taken to 83% and 93% conversion, and the unreacted **3** was recovered by an extractive workup followed by flash chromatography. The samples of recovered **3** were analyzed by ¹³C NMR, along with standard samples that had not been subjected to the reaction conditions. The change in isotopic composition in each position was determined relative to the meta carbons of the phenyl ring,¹² with the assumption that isotopic fractionation of this position was negligible. From the percentage conversions and the changes in isotopic composition, the KIEs were calculated as previously described.¹¹

The results are shown in Figure 1. The independent sets of ¹³C KIEs agree within the standard deviation of the measure-

- (6) (a) Bach, R. D.; Glukhovtsev, M. N.; Gonzalez, C.; Marquez, M.; Estevez, C. M.; Baboul, A. G.; Schlegel, H. B. *J. Phys. Chem. A* **1997**, *101*, 6092–6100. (b) Houk, K. N.; Liu, J.; DeMello, N. C.; Condroski, K. R. *J. Am. Chem. Soc.* **1997**, *119*, 10147–10152. (c) Crehuet, R.; Anglada, J. M.; Cremer, D.; Bofill, J. M. *J. Phys. Chem. A* **2002**, *106*, 3917–3929. (d) Bach, R. D.; Dmitrenko, O.; Adam, W.; Schambony, S. *J. Am. Chem. Soc.* **2003**, *125*, 924–934.
- (7) Dmitrenko, O.; Bach, R. D. *J. Phys. Chem. A* **2004**, *108*, 6886–6892.
- (8) For a study of epoxidations with fluorinated dioxiranes, see: Armstrong, A.; Washington, I.; Houk, K. N. *J. Am. Chem. Soc.* **2000**, *122*, 6297–6298.
- (9) (a) Baumstark, A. L.; McCloskey, C. J. *Tetrahedron Lett.* **1987**, *28*, 3311–3314. (b) Yang, D.; Wang, X.-C.; Wong, M.-K.; Yip, Y.-C.; Tang, M.-W. *J. Am. Chem. Soc.* **1996**, *118*, 11311–11312.

- (10) (a) Okovytyy, S.; Gorb, L.; Leszczynski, J. *Tetrahedron Lett.* **2002**, *43*, 4215–4219. (b) For a strong countering study, see: Bach, R. D.; Dmitrenko, O. *J. Phys. Chem. A* **2003**, *107*, 4300–4306.

- (11) Singleton, D. A.; Thomas, A. A. *J. Am. Chem. Soc.* **1995**, *117*, 9357–9358.

- (12) The meta carbon of **3** is more separate from other peaks in the ¹³C NMR than the para carbon, and its use as standard gives lower variance in the isotope effects than when the para carbon is used as standard. Both meta and para carbons are computationally predicted to exhibit a ¹³C KIE of unity, and each exhibit ¹³C KIEs within experimental error of unity relative to the other.

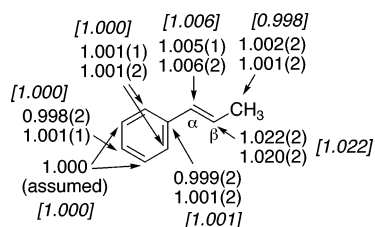


Figure 1. Experimental and predicted ^{13}C KIEs ($k_{12\text{C}}/k_{13\text{C}}$) for the epoxidation of **3** catalyzed by **1** at 0°C . The two sets of experimental KIEs refer to two independent experiments, and standard deviations in the last digit from six determinations are shown in parentheses. The predicted ^{13}C KIEs are shown in italics and brackets and are based on transition structure **10**.

ments, with the exception of the para-carbon's KIEs. Such a minor disagreement could simply be the result of random error. Only the C_β and C_α KIEs differ significantly from unity, with a relatively large C_β isotope effect and a much smaller KIE at C_α . These KIEs qualitatively indicate a significantly asynchronous transition state for the epoxidation, with more advanced formation of the incipient $\text{C}_\beta\text{--O}$ bond than the $\text{C}_\alpha\text{--O}$ bond. A more quantitative interpretation of these KIEs will be possible with the aid of theoretical calculations.

Theoretical Calculations. The theoretical study of this reaction is complicated by the size of the system, the possible involvement of several conformations of **5**, and the many possible orientations for approach of the alkene. The conformations of **5** were first studied by carrying out a molecular dynamics search for conformers using an MM2 force field. Candidate structures were then optimized using B3LYP calculations with a 6-31G* basis set, and single-point energies using a 6-311+G** basis set were obtained for each optimized structure. A total of six conformers of **5** were identified for further study (see Supporting Information for full geometries), arising from the combination of a chair and two boat conformations for the pyran b ring with two conformers each in the spiro dioxolane ring (ring c). The structures **5-chair** and **5-boat** are drawn to depict the calculated geometries for the lowest-energy chair and boat structures. Interestingly, **5-boat** is predicted to be only 2.3 kcal/mol above **5-chair** (B3LYP/6-311+G**//B3LYP/6-31G* + zpe), so its reactive importance cannot be readily dismissed.

A variety of combinations of the six conformers of **5** with intuitively rational possibilities for approach of the alkene were then explored in B3LYP/6-31G* calculations in a search for transition structures. In this way, a total of 18 epoxidation transition structures were located. The eight structures **10–17** that were predicted to be lowest in energy are shown in Figure 2; the remaining structures are shown in the Supporting Information. It should be noted that a great many possibilities were left unexplored; we estimate that a total of 66 transition structures might have been located. The 18 structures located all lie within an ~ 8 kcal/mol range, and it would be difficult to argue convincingly from theory alone that the best transition structure had been found.

To evaluate the experimental relevance of these structures and interpret the observed isotope effects, ^{13}C KIEs were predicted for each of the transition structures. These predictions

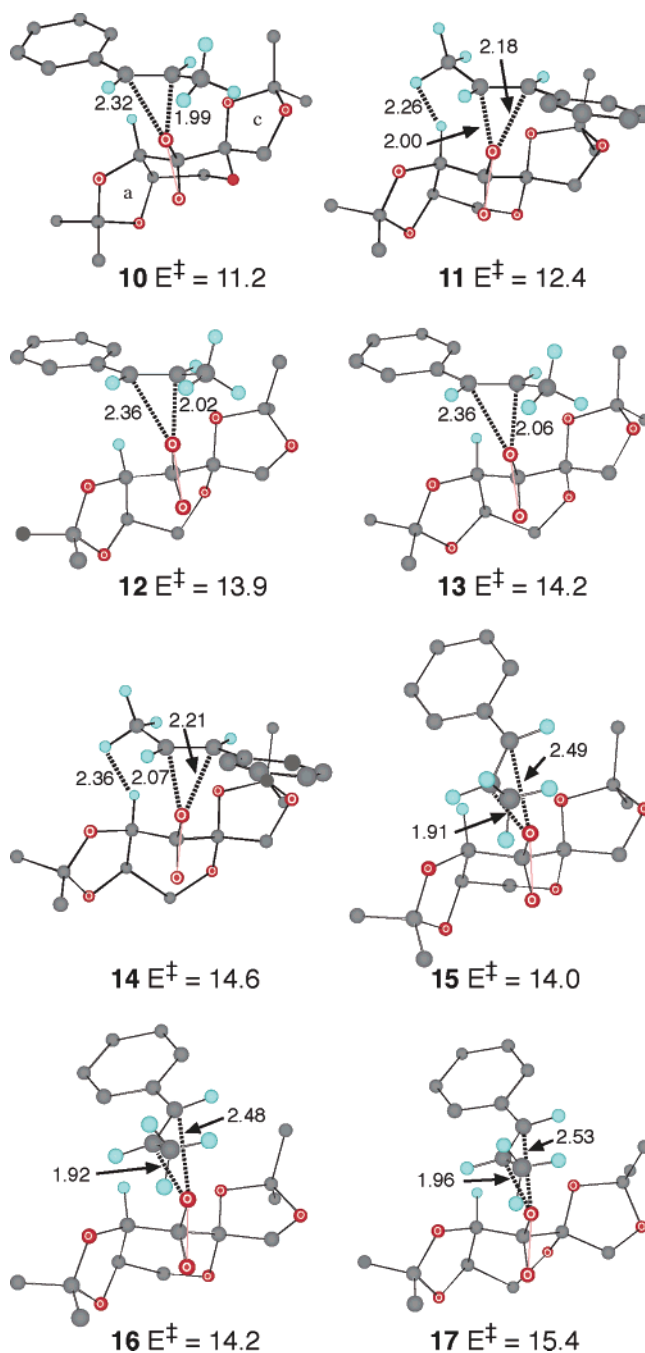


Figure 2. Calculated transition structures for the epoxidation of **3** by **5**. Most hydrogens have been removed for clarity. Energies are B3LYP/6-311+G**//B3LYP/6-31G* + zpe reaction barriers in kcal/mol. Stereoviews and 10 additional structures are given in the Supporting Information.

used the scaled theoretical vibrational frequencies¹³ in conventional transition state theory by the method of Bigeleisen and Mayer.¹⁴ Tunneling corrections were applied using a one-dimensional infinite parabolic barrier model.¹⁵ Such KIE predictions including a one-dimensional tunneling correction have proven highly accurate in reactions not involving hydrogen transfer, so long as the calculation accurately depicts the mechanism and transition state geometry.¹⁶ The KIEs based on

(13) The calculations used the program QUIVER (Saunders, M.; Laidig, K. E.; Wolfsberg, M. *J. Am. Chem. Soc.* **1989**, *111*, 8989–8994). Frequencies were scaled by 0.9614.

(14) (a) Bigeleisen, J.; Mayer, M. G. *J. Chem. Phys.* **1947**, *15*, 261–267. (b) Wolfsberg, M. *Acc. Chem. Res.* **1972**, *5*, 225–233. (c) Bigeleisen, J. *J. Chem. Phys.* **1949**, *17*, 675–678.

(15) Bell, R. P. *The Tunnel Effect in Chemistry*; Chapman & Hall: London, 1980; pp 60–63.

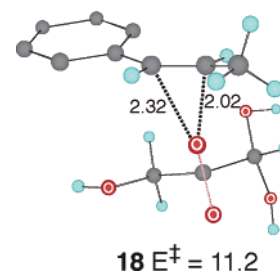
the lowest-energy transition structure **10** are shown in Figure 1, and the predicted KIEs for the remaining transition structures are shown in the Supporting Information.

The agreement between the experimental and predicted KIEs is striking. With the exception of the β -methyl group, all of the predicted isotope effects are within the uncertainty of the experimental measurement. The agreement of experiment and theory for C_β and C_α in particular supports the accuracy of the calculations with regard to the asynchronicity of the oxygen transfer. Notably, the comparison of experimental and predicted KIEs also excludes most of the calculated transition structures, as 15 of the 18 transition structures lead to KIE predictions for C_β and/or C_α that are outside of experimental error. (See the Supporting Information.) For example, structure **11** has a relatively short C_α -O distance of 2.18 Å, and its predicted C_α KIE of 1.009 is too large. Only structures **10**, **12**, and **13** lead to accurate KIE predictions. The C_β and C_α KIEs appear to be very sensitive functions of the asynchronicity; there is a consistent structural trend in the predicted isotope effects in which shorter C_β -O or C_α -O distances in the transition structures are associated with larger predicted ^{13}C KIEs. The asynchronicity varies greatly among the diverse structures, and only **10**, **12**, and **13** appear to approximate the actual asynchronicity well.

The two lowest-energy transition structures **10** and **11** were reoptimized using a 6-31+G** basis set. This led to a very slight (0.01–0.03 Å) lengthening of the C_β -O and C_α -O distances but otherwise the geometries are changed little. The predicted barriers with these fully optimized structures are 11.4 and 12.7 kcal/mol, very close to the single-point barriers in Figure 2. The predicted KIEs for **10** change in each case by less than 0.0004.

Given the experimental support for the approximate accuracy of the calculational methodology, the nature of structural effects impacting the enantioselectivity can now be considered. It should be noted for further consideration that the asynchronicity in **10**, **12**, and **13** closely resembles that found in transition structure **18** for reaction of **3** with a trihydroxy analogue of dimethyldioxirane. Considering **18** as a model for an unhindered epoxidation, the asynchronicity in **18** may be considered as the “natural” asynchronicity. In this case, the unsymmetrical alkene **3** favors having a longer partial C–O bond adjacent to the phenyl group. With a simple symmetrically substituted alkene such as *trans*-2-butene, the natural asynchronicity is very low; the predicted transition structure has nearly equal C–O distances for the olefinic carbons (see the Supporting Information). When compared to **18**, the alkenyl moieties of **10**, **12**, and **13** are slightly pushed away from the dioxolane c ring, but otherwise the chiral environment of **5** allows the natural asynchronicity in these structures. In the other transition structures, **5** imposes “unnatural” asynchronicity. Any transition state is inherently flexible, and epoxidations with dioxiranes are thought to involve a particularly soft potential energy surface,⁷ but departure from the natural transition state geometry necessarily imparts an

energy cost. This idea provides a simple intuitive framework for understanding effects on the selectivity in these reactions.



Structures **10–14** would afford the major enantiomeric product, while **15–17** would afford the minor enantiomer. All of the structures giving the major enantiomer are spiro and place a hydrogen toward the most hindered quadrant containing the dioxolane c ring. This supports Shi's previous analysis.² A surprising result, however, is the substantial preference for structure **10** over **11**. This results from the asynchronicity of the transition structures. In **10**, the phenyl group of **3** is positioned toward the α hydrogen on the pyran ring, but because the phenyl group is adjacent to the relatively long incipient C_α -O bond, there is little steric interaction. In **11**, the methyl group of **3** is positioned toward the α hydrogen on the pyran ring. Because the methyl group is adjacent to the relatively short C_β -O bond, an unfavorable methyl/H steric interaction results. To minimize this interaction, **11** is less asynchronous than “natural,” and this is disfavored.

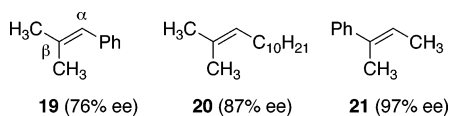
The transition structures **15–17** leading to the opposite enantiomer are neither spiro nor planar; rather, the plane of the incipient epoxide ring is twisted at roughly 45° from the plane of the dioxirane, and the asynchronicity of the transition structures is increased. The combination of the twisting and greater asynchronicity has the effect of minimizing a steric interaction of the phenyl group with the methyls of the dioxolane c ring. An alternative transition structure in which the methyl and phenyl groups of **15** are exchanged in position (see structure C in the Supporting Information) is 2.5 kcal/mol higher in energy; this structure has the same problem as **11** in that the natural asynchronicity, with a short C_β -O bond, would greatly increase steric interaction with the dioxolane. Structure **16** differs from **15** only by the conformation of the dioxolane c ring, while **17** has a boat conformation in the pyran ring. The boat transition structures **12** and **13** are sterically similar to **10** and are higher in energy by amounts that mainly reflect the ground-state boat/chair energy difference in **5**.

The asynchronicity effect that disfavors transition structure **11** in the epoxidation of **3** has no outward consequence because the major enantiomer can be formed via **10**. In other cases, however, this effect appears to have an impact. One interesting observation is that the ee for **19** is relatively low while a higher ee is obtained with **20** and a very high ee is observed with **21**.^{3b} This trend may be understood by considering the facility of formation of the major enantiomer.¹⁷ In the case of **19**, the asynchronicity would be such that a relatively short C_β -O bond would be favored at the transition state, but this would force the *trans* methyl group into a sterically bad position (identical

(16) (a) Beno, B. R.; Houk, K. N.; Singleton, D. A. *J. Am. Chem. Soc.* **1996**, *118*, 9984–9985. (b) Meyer, M. P.; DelMonte, A. J.; Singleton, D. A. *J. Am. Chem. Soc.* **1999**, *121*, 10865–10874. (c) DelMonte, A. J.; Haller, J.; Houk, K. N.; Sharpless, K. B.; Singleton, D. A.; Strassner, T.; Thomas, A. A. *J. Am. Chem. Soc.* **1997**, *119*, 9907–9908. (d) Singleton, D. A.; Merrigan, S. R.; Liu, J.; Houk, K. N. *J. Am. Chem. Soc.* **1997**, *119*, 3385–3386.

(17) Of course, the observed ee depends equally on the facility of formation of the minor enantiomer, but this is less obviously affected by the substitution patterns in **19–21**.

to that in **11**). In **20**, the asynchronicity of the transition state should be decreased, decreasing the steric interaction with the trans methyl group. In **21**, a phenyl group is forced toward the pyran ring, but, as in **10**, the adjacent incipient C–O bond would be long at the transition state and there would be little steric interaction between the phenyl group and the pyran.



cis-Alkenes and Terminal Alkenes. The major enantiomeric product in the reaction of *trans*-disubstituted or trisubstituted alkenes catalyzed by **1** arises from a spiro transition state transferring the equatorial oxygen, as Shi has proposed.² However, when this model is applied to epoxidations of *cis*-disubstituted and terminal alkenes using **2b**, the two transition states **8** and **9** affording opposite enantiomers would seem equally good. Why would the predominant product arise from **8** in which the π -conjugating substituent is oriented proximal to the oxazolidinone ring?

We first sought to find out if this preference could be reproduced in a calculational model. This was not obvious; if the preference arises from an attractive interaction due to a dispersion force, such interactions are not well reproduced by DFT calculations. To examine this issue, transition structures were located for the epoxidation of styrene and *cis*- β -methylstyrene with the dioxirane derived from **2b** (R = CHO). Our studies with these alkenes were limited to the chair conformation of the dioxirane and reaction of the equatorial oxygen, as in the Shi conception. This is an incomplete examination, but based on the results with **1**, it should be sufficient to identify the major effects on the stereochemistry.

The four lowest-energy transition structures **22**–**25** located for the epoxidation of styrene catalyzed by **2b** are shown in Figure 3. Two transition structures closely analogous to **22** and **23** for the epoxidation of *cis*- β -methylstyrene are shown in the Supporting Information, along with an additional higher-energy transition structure with styrene. The lowest-energy transition structure **22** corresponds to **8** and would afford the observed major product. The predicted preference for the major enantiomer, at 1.4 kcal/mol, fits well with the experimental product ratio of approximately 9:1.5. Transition structure **23**, corresponding to **9**, would afford the minor enantiomeric product, as would the alternative transition structure **25**. Interestingly, **25**, which places the phenyl group in what would be expected to be the most sterically hindered position toward the oxazolidinone ring, is similar in energy to **23** and **24**. (A transition structure analogous to **25** for the reaction of **3** with **5** (Supporting Information) was prohibitively high in energy.) Another surprise is that **24**, corresponding to the best transition structure **10** when **1** was the catalyst, is predicted to be significantly higher in energy than **22**.

The calculations correctly predict the major enantiomeric product (this is also true with *cis*- β -methylstyrene; see Supporting Information), but the qualitative understanding of the enantioselectivity is a more difficult and subtle issue. One apparent contributing factor to the preference for **22** over **23** and **24** is that the asynchronicity of the transition structures in **23** and **24** forces an olefinic hydrogen into a steric interaction

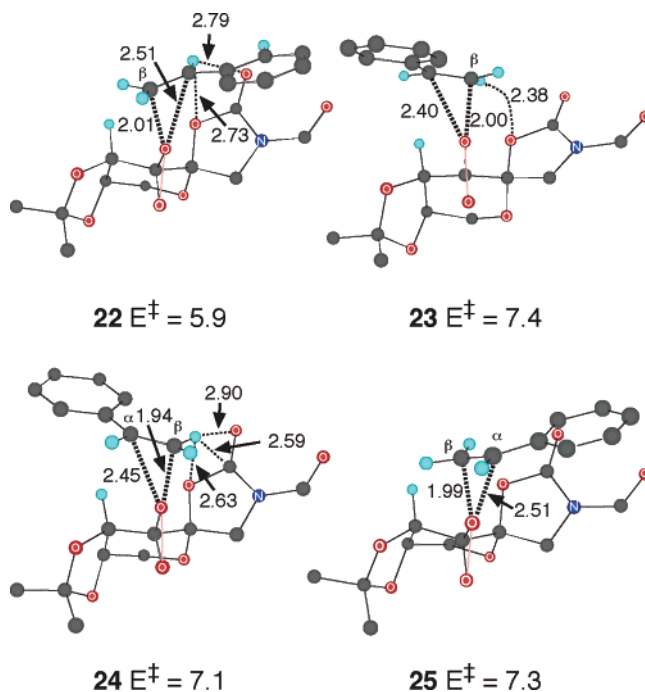


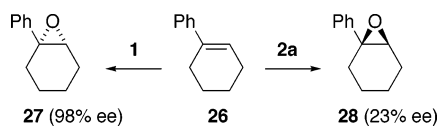
Figure 3. Calculated transition structures for the epoxidation of styrene by the dioxirane derived from **2b**. Most hydrogens have been removed for clarity. Energies are B3LYP/6-311+G**//B3LYP/6-31G* + zpe reaction barriers in kcal/mol. One additional higher-energy structure is shown in the Supporting Information.

with the oxazolidinone ring. Model calculations using ethylene and oxazolidinone suggest that the minimum-energy distance for interaction of an olefinic hydrogen with the ring oxygen of oxazolidinone is about 2.8 Å. This is approximately what is found in **22**, but in **23** and **24** the H–O distance is too short (see Figure 3). As is normal for steric interactions, the effect is distributed into other distortions in the transition structures. For example, the approach of the alkene in **23** and **24** is “pushed” away from the oxazolidinone, so that the C_{β} –O–O angle in each is 166°. For comparison, the C_{β} –O–O angle is only 160° in both **22** and in an unstrained model (analogous to **18**, only using styrene instead of **3**; see Supporting Information). The “reversed” asynchronicity in **25** as compared to **23** and **24**, as well as a twist of the transition state away from spiro by about 45°, minimizes the steric interaction of the phenyl group with the oxazolidinone. As a result, the phenyl/oxazolidinone steric interaction in **25** seems to have no more direct effect than the hydrogen/oxazolidinone interaction in **23** and **24**.

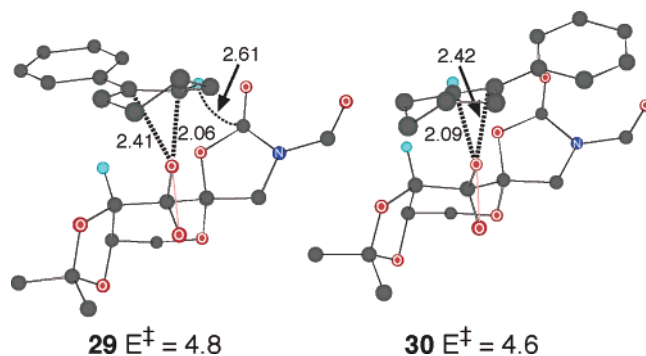
Another factor that appears to be contributing to the preference for **22** and the relatively low energy of **25** is a dipolar interaction. Epoxidation with dioxiranes is an electrophilic process, and there is a partial positive charge developed in the styrene moiety at the transition state. For example, the total Mulliken charge in the styrenyl part of **22** is 0.33. There is a dipole associated with the oxazolidinone ring, and this dipole would be oriented so as to stabilize **22** and **25** relative to **23** and **24**. In **25** in particular, the partially positive phenyl ring is approaching the partially negative oxazolidinone oxygens.

Consideration of the factors affecting the stability of **22**–**25** aids in the understanding of enantioselectivity in related reactions. Shi has made the interesting observation that 1-phenylcyclohexene (**26**) affords high selectivity for the (*R,R*) product **27** with **1** as catalyst but low selectivity for the opposite

enantiomer with **2a** as catalyst.² Additionally, substituents on the oxazolidinone nitrogen have a significant impact on the enantioselectivity. With **1**, a transition structure similar to **10** should be heavily favored, as was true with **21** above. With **2a** as catalyst, however, transition structures analogous to **22** and **23** would be precluded because they place the cyclohexenyl ring in an unfavorable position toward the pyran. The expected lowest-energy transition structures would be analogues of **24** and **25**.



Based on this prescription, transition structures **29** and **30** were located for the epoxidation of phenylcyclohexene catalyzed by **2b**. The preferred transition structure **30** would afford **28**, and the small preference for **30** over **29** of 0.2 kcal/mol is well consistent with experimental observations. The structures of **29** and **30** support the ideas discussed with **22**–**25**. Although the phenyl group of **29** is well positioned to avoid steric interactions, the asynchronicity of the transition structure appears to push the olefinic hydrogen of **29** too close to the oxazolidinone. In contrast, the asynchronicity of **30** minimizes steric interactions between the phenyl group and the oxazolidinone. An additional interesting effect in **30** is that the phenyl group is twisted away from conjugation with the olefin by 28°, as compared to 0°–10° with **22**–**25**. It would seem that for the epoxidation of this trisubstituted alkene, activation by conjugation with the phenyl group is of decreased importance, allowing the phenyl group to twist so as to minimize steric interactions. Because the phenyl group in **30** is still pushed up against the oxazolidinone ring, the relatively large effect of substituents on the nitrogen is understandable. It should be noted that, aside from the impact of asynchronicity on steric interactions, the basic analysis here is quite similar to the qualitative analysis described by Shi.²



Conclusions

The potential energy surface for the epoxidation of alkenes with dioxiranes is thought to be very soft.⁷ Under these circumstances, even very high level calculations cannot unambiguously decide between synchronous and asynchronous transition states for reactions of simple alkenes with simple dioxiranes, and the adequacy of a DFT method applied to a large enantioselective reaction cannot be assured theoretically. However, the calculated ¹³C KIEs for diverse epoxidation transition structures suggest that the observed isotope effects should be a very sensitive measure of the transition state geometry. The

experimental KIEs match well with those predicted for the lowest-energy theoretical transition structure **10**. This supports the approximate accuracy of **10** and by implication supports the applicability of B3LYP/6-31G* calculations to these reactions. Multireference methods appear unnecessary here for geometrically accurate transition structures.^{7,10}

The transition state for epoxidation of *trans*- β -methylstyrene catalyzed by **1** is asynchronous with a shorter incipient C β –O bond at the transition state. This asynchronicity approximates that in an unstrained model, and the asynchronicity of such unsymmetrical reactants is expected to have consequences. High enantioselectivity should be promoted when the major enantiomer can arise by a transition state for which the catalyst allows the natural asynchronicity. In contrast, when the natural asynchronicity of the epoxidation is hindered by the catalyst, as in the case of **19**, the enantioselectivity will likely be lowered.

The asynchronicity of transition states for unsymmetrical reactants has a significant impact on steric interactions at the transition state. Asynchronicity in the “wrong” direction, as in **23**, **24**, and **29**, increases steric interactions, while asynchronicity in the right direction decreases them, as in **22**, **25**, and **30**. The consideration of such an effect of asynchronicity is necessary to understand the significant preference for π -conjugating substituents to be proximal to the oxazolidinone of **2a** in the literature observations. Overall, the asynchronicity of transition states for epoxidations by dioxiranes must be considered carefully in efforts to understand enantioselectivity in these reactions.

Experimental Section

Epoxidation of 3 Catalyzed by 1. All glassware used for the reaction was washed carefully to remove trace of metals, which catalyze the background reaction and lead to lower enantioselectivity. A mixture of 3.54 g (30 mmol) of **3**, 0.41 g (3 mmol) of 1,4-dimethoxybenzene (internal standard), 450 mL of a 1:2 mixture of acetonitrile and dimethoxymethane, 300 mL of buffer solution (0.05 M solution of Na₂B₄O₇·10H₂O in 4 × 10^{−3} M aqueous Na₂(EDTA)), 0.34 g (1 mmol) of tetrabutylammonium hydrogen sulfate (phase transfer catalyst), and 1.55 g (6 mmol) of **1** was cooled with an ice bath, and solutions of 50 g (81 mmol) of Oxone in 390 mL of 4 × 10^{−3} M aqueous Na₂(EDTA) and 390 mL of 0.89 M K₂CO₃ were added dropwise separately and simultaneously during a period of 1.5 h. The reaction mixture was then stirred for another 30–60 min before the reaction was quenched by addition of 1 L of water. The resulting mixture was extracted with three portions of 100 mL of pentane, and the combined organic layers were washed with three portions of 100 mL of brine, and dried over Na₂SO₄. The solvent was removed under vacuum, and the conversion was determined based on the ¹H NMR integration of olefin protons in *trans*- β -methylstyrene (at δ 6.15 and δ 6.37) versus the methoxy signal in the internal standard. The unreacted **3** was then recovered by a flash silica gel column eluted with a 95:5 mixture of hexane/dichloromethane. By this procedure, two identical reactions were taken to 83% and 93% conversion and afforded 495 and 220 mg of recovered **3**, respectively.

NMR Measurements. All samples were prepared using a constant 220 mg of **3** in 5 mm NMR tubes filled with CDCl₃ to a constant height of 5.0 cm. The ¹³C spectra were recorded at 125.70 MHz using inverse gated decoupling, 110 s delays between calibrated $\pi/2$ pulses, and a 6.560 s acquisition time to collect 262 144 points. Integrations were numerically determined using a constant integration region for each peak. A zero-order baseline correction was generally applied, but no first-order correction was applied. Six spectra were recorded for each sample of recovered *trans*- β -methylstyrene along with samples of *trans*- β -methylstyrene, which were not subjected to the reaction

conditions. The resulting ^{13}C integrations for the spectra are provided in the Supporting Information. The KIEs were calculated as previously described.¹¹

Acknowledgment. We are thankful for NIH grant # GM-45617 and to The Robert A. Welch Foundation for support of this research.

Supporting Information Available: Energies and full geometries of all calculated structures and NMR integration results for all reactions. This material is available free of charge via the Internet at <http://pubs.acs.org>.

JA0435788